Polychromatic Image Performance of Diffractive Bifocal Intraocular Lenses: Longitudinal Chromatic Aberration and Energy Efficiency

María S. Millán, Fidel Vega, and Inmaculada Ríos-López

Departament d'Òptica i Optometria, Universitat Politècnica de Catalunya, BARCELONATECH, Terrassa, Spain

Correspondence: María S. Millán, Departament d'Òptica i Optometria, Universitat Politècnica de Catalunya, BARCELONATECH, Violinista Vellsolà 37, 08222 Terrassa, Spain; millan@oo.upc.edu.

Submitted: December 11, 2015
Accepted: March 11, 2016

Citation: Millán MS, Vega F, Ríos-López I. Polychromatic image performance of diffractive bifocal intraocular lenses: longitudinal chromatic aberration and energy efficiency. *Invest Ophthalmol Vis Sci*. 2016;57:XXX–XXX. DOI:10.1167/iovs.15-18861

Purpose. The study evaluated—theoretically and experimentally—the longitudinal chromatic aberration (LCA) and through-focus energy efficiency (TF-EE) of diffractive–refractive bifocal intraocular lenses (2f-IOLs).

Methods. Four aspheric 2f-IOLs (Tecnis +4.00 diopter [D] ZMA00, +2.75 D ZKB00, and AcrySof +4.0 D SN6AD3, +2.5 D SV25T0) of same base power 30 D, but different design, additional power, and different material, were tested in vitro in terms of TF-EE when illuminated by 3 red ($\lambda_R = 625$ nm), green ($\lambda_G = 530$ nm), and blue ($\lambda_B = 455$ nm) lights. The LCA affecting the distance and near foci was derived theoretically and measured experimentally from the contributions of the IOLs' refractive and diffractive powers. Longitudinal chromatic aberration was evaluated in a pseudophakic schematic eye.

Results. The distance focus of all 2f-IOLs showed lower energy efficiency (EE) for the blue than for the red light. AcrySof IOLs showed the largest amount of positive LCA in the distance focus that, combined with corneal LCA, would increase the resulting distance LCA in a pseudophakic eye. The near focus of all 2f-IOLs showed higher EE for the blue than for the red light. Better compensation for the LCA of a pseudophakic eye at near focus is obtained with Tecnis than with AcrySof 2f-IOLs.

Conclusions. The energy distribution between the foci of diffractive 2f-IOLs depends on the lens design, the illumination wavelength, and to a lesser extent, the additional power. In distance vision, 2f-IOLs' refractive base power increases the positive LCA of prior ocular media, and the resulting LCA may even surpass the natural LCA of human eye. In near vision, however, the achromatizing effect of diffractive 2f-IOLs may compensate, in part, the natural eye's LCA.

Keywords: chromatic dispersion, cataract, intraocular lens, multifocal intraocular lens, diffractive lens, longitudinal chromatic aberration, image quality, optical testing, optical material

A diffractive bifocal intraocular lens (2f-IOL) typically uses a hybrid diffractive-refractive design that consists of a high-power refractive base lens (similar to that considered for a monofocal design) and an additional (add) low-power diffractive profile engraved on either the front (e.g., AcrySof ReSTOR; Alcon Laboratories, Inc., Duluth, GA, USA) or the back surface of the lens (e.g., Tecnis; Abbott Medical Optics, Inc., Santa Ana, CA, USA). This diffractive profile mainly utilizes the zero and the first diffraction orders to produce two images: The zero-order energy directs to the distance image formed by the high-power refractive base lens, whereas the first-order energy directs to the near image formed by the combined base plus add powers. Many IOL designs also include compensation for the positive spherical aberration of the cornea to some extent.[1]

Under white light illumination, the distance image formed by a 2f-IOL is affected by the longitudinal chromatic aberration (LCA) of the refractive part of the hybrid lens, which depends on its base power and the dispersive properties of its optical material (i.e., through the variation of the refractive index with wavelength). This aberration is of the same sign as that in the human eye. The LCA of the near image, however, has the additional contribution of a term of opposite sign—due to the diffractive element—that can be relevant, depending on the add-power value. After implanting a 2f-IOL in the human eye, the final LCA of the distance and near images resulted from the further contributions of other components of the eye (cornea, aqueous and vitreous humors). In addition to LCA, the energy distribution between the distance and near images of diffractive 2f-IOLs also shows a strong dependency on wavelength.[2,3]

In this work, we studied and measured the chromatic properties of 4 aspheric diffractive 2f-IOLs (2 nonapodized and 2 apodized of different add power) using an experimental setup arranged on an optical bench. Two monofocal (1f-IOL) counterparts (Tecnis model ZA9003, from Abbott Medical Optics, and AcrySof model SN60WF, from Alcon) of the nonapodized and apodized 2f-IOLs, with similar base power, aspheric design, and material, also have been included as references in our study. Three light-emitting diodes (LEDs) with emission in the blue (B), green (G), and red (R) spectral bands have sequentially illuminated the setup. More specifically, we measured through-focus energy efficiency (TF-EE) of the IOLs with the R, G, and B lights and LCA in both the near (LCA_N) and the distance (LCA_D) foci of the lenses experimentally obtained

Investigative Ophthalmology & Visual Science

?15

Table 1. Technical Specifications of the 2f-IOLs and Reference 1f-IOLs Under Study as Provided by the Manufacturer[9,11]

	Model and Manufacturer					
	Tecnis, Abbott Medical Optics			AcrySof IQ, Alcon Laboratories		
	ZMA00	ZKB00	ZA9003	ReSTOR SN6AD3	ReSTOR SV25T0	SN60WF
Material	Hydrophobic acrylic			Acrylate/methacrylate copolymer		
Refractive index n	1.47	1.47	1.47	1.55	1.55	1.55
Abbe value V	55	55	55	37	37	37
Color filter	UV blocking	UV blocking	UV blocking	UV and blue light	UV and blue light	UV and blue light
Optic design	Full aperture Posterior	Full aperture Posterior		Apodized Anterior	Apodized Anterior	
ϕ_{Diff}, mm				3.6	3.6	
Aspheric surface*	Anterior	Anterior	Anterior	Anterior	Anterior	Anterior
$SA = c[4,0]$, μm	−0.27	−0.27	−0.27	−0.1	−0.2	−0.2
Base power, D	30	30	30	30	30	30
Add power at IOL plane, D	+4.0	+2.75	-	+4.0	+2.5	-
At spectacle plane	+3.0	+2.01	-	+3.2	+2.0	-
Energy distribution Distance/near, %	40/40	40/40	-	70/20†	77/13†	-

The refractive index assumes a wavelength of 555 nm and the IOL inserted in the eye (37°C).
* Data for a 6-mm pupil.
† Data from the specification sheet curves for a 3.5-mm pupil.

from the previous through-focus analysis. Mathematical expressions to calculate the LCA in both foci have been also derived.

To isolate the LCA and other effects produced by a 2f-IOL in the distance and near foci, the IOL was introduced in a wet cell. By doing so, all the refractive and diffractive power was exclusively due to the IOL. The optical setup was similar to that used by the authors in related works and described in detail elsewhere,[4,5] except for the artificial cornea, which was removed from the setup in this experiment. Once the TF-EE and LCA measurements were taken, we additionally set the IOL virtually in a pseudophakic schematic eye (Le Grand eye),[6] which provided the average refractive characteristics of other ocular media (cornea, aqueous and vitreous humors) and computed closer estimates for the LCA in the human eye.

Related research has been extensively developed and reported using different IOL designs and model eyes. It is worth mentioning some closely related works (see Refs. 2, 7, 8); their analyses and numerical simulations have provided a valuable background to our work. However, some of their assumptions meant their methods were not fully applicable to our study on diffractive 2f-IOLs of different material, add power, and design (for more details, see the Discussion section). Thus, we have considered the refractive characteristics of the hybrid IOL (i.e., refractive power and dispersion) as contributions separate from those of the cornea and ocular humors. Our polychromatic analysis and experimental through-focus results show the IOLs' own contribution to the chromatic aberration in the far as well as in the near focus of a pseudophakic schematic eye implanted with such a lens. These results allow us to further compare the experimental chromatic performance of the studied aspheric IOLs (4 diffractive bifocals and 2 reference monofocals) in terms of TF-EE and LCA, something that is more commonly treated just theoretically or by numerical simulation.[2,8]

Materials and Methods

Intraocular Lenses

Six IOLs were used in the experimental work of this study. Their technical specifications are listed in Table 1. AcrySof ReSTOR[9] 2f-IOLs have an apodized diffractive design, that is, with steps of decreasing height from center to periphery. The diffractive zone covers the central part (3.6-mm diameter) of the anterior aspheric surface and is surrounded by a peripheral ring that is purely refractive. This design aims at directing a higher amount of the incoming energy to the distance focus with enlarged pupils and, therefore, reducing more effectively the formation of halos in distance vision.[10] Tecnis[11] 2f-IOLs have a posterior spherical surface with a nonapodized diffractive design that fully covers its aperture. This design is intended to produce a balanced distribution of energy between the distance and the near foci independently of the pupil diameter.

All the IOL lenses considered in this study have an aspheric surface, designed to compensate to some extent for the natural positive spherical aberration (SA) of the human cornea. Table 1 shows the SA values in terms of the c[4,0] Zernike coefficient for a 6-mm pupil diameter.

The tested IOLs are made of dispersive optical materials that show different refractive indexes and Abbe values (Table 1). AcrySof IOLs have higher refractive index and show greater dispersion (lower Abbe value) than Tecnis IOLs, but on the other hand, they allow the design of thinner lenses, which is an advantageous property in the surgical practice because thinner lenses require smaller incisions.

In addition to the standard UV light (<400 nm) filtering exhibited by all the tested IOLs, AcrySof IOLs have a blue-light filtering chromophore that reduces the transmittance of blue light wavelengths (400–475 nm), giving them a yellowish appearance.

Longitudinal Chromatic Aberration of a Refractive–Diffractive Thin Lens

Longitudinal chromatic aberration is given by the variation in the focal length f or, equivalently, in the optical power P with the illuminating wavelength λ. This variation is caused by the dispersive nature of optical materials, whose refractive index n also exhibits wavelength dependency. The Abbe value (V), also called Abbe number, is widely used to characterize the dispersion of an optical material. It is defined as $V = [n(\lambda_d) - 1] / [n(\lambda_F) - n(\lambda_C)]$, where $\lambda_F = 486$ nm, $\lambda_d = 588$ nm, and $\lambda_C =$

656 nm. The refractive power of a thin lens of refractive index $n_L(\lambda)$ immersed in a medium of refractive index $n_A(\lambda)$ is given by

$$P_R(\lambda) = \frac{n_A(\lambda)}{f(\lambda)} = (n_L[\lambda] - n_A[\lambda])K, \quad (1)$$

where K is a geometrical constant of the thin lens involving its front r_1 and back r_2 radii ($K = 1 / r_1 - 1 / r_2$). .We recall that although the aqueous and vitreous humors are different media, their refractive indexes are close, and that is why, in a first approach and for the sake of simplicity, they are considered to have similar value in many studies. We do the same in this work by considering the IOL immersed in a medium with refractive index $n_A(\lambda)$. Since the refractive index $n(\lambda)$ of optical materials typically decreases when the wavelength increases, Equation 1 implies that a thin lens shows lower refractive power for longer wavelengths (i.e., $P_R[\lambda_C] < P_R[\lambda_F]$). The LCA in the focal plane of the thin lens can be estimated from the variation of the refractive power ΔP_R corresponding to F and C wavelengths, that is, $\Delta P_R\{\text{FdC}\} = P_R(\lambda_F) - P_R(\lambda_C)$. Taking into account Equation 1 and the definition of the Abbe value, the following expression for ΔP_R can be obtained:

$$\Delta P_R\{\text{FdC}\} = \left(\left[\frac{n_L(\lambda_d) - 1}{V_L}\right] - \left[\frac{n_A(\lambda_d) - 1}{V_A}\right]\right) \times \frac{P_R(\lambda_d)}{n_L(\lambda_d) - n_A(\lambda_d)}. \quad (2)$$

Equation 2 is the LCA corresponding to the single focus of a 1f-IOL intended for distance vision exclusively. In the case of a diffractive 2f-IOL whose refractive–diffractive design produces 2 main foci at the zero and first diffraction orders, Equation 2 corresponds to the LCA in the zero-order focus or, in other terms, at the distance focus

$$\text{LCA}_D = \Delta P_R. \quad (3)$$

Note that the power variation of Equation 2 depends linearly on the design power of the refractive base lens. It also depends on the wavelength change through the refraction indexes, which is a variation relatively slower than the one produced in a diffractive lens, as we will see next.

Let us denote by $P_{\text{Da}}(\lambda_0)$ the diffractive add power for the first diffraction order at the design wavelength λ_0. This power in diopters (D) is given by $\text{P}_{\text{Da}}(\lambda_0) = 2\text{m}\lambda_0 / r_m^2$, where r_m indicates the radius of the m^{th} zone in meters and the design wavelength λ_0 is expressed in meters too.[12] The variation of wavelength entails a variation in the diffractive add power given by

$$\Delta P_{\text{Da}}\{\lambda\} = -\frac{\Delta\lambda}{\lambda_0} P_{\text{Da}}(\lambda_0). \quad (4)$$

This variation depends linearly on both the wavelength change $\Delta\lambda$ and the design add power P_{Da} of the diffractive part. Equation 4 involves a much faster variation of the diffractive add power with wavelength than the refractive base power (Equation 2). The negative sign in Equation 4 accounts for a variation in opposite direction: The diffractive add power is then higher for longer wavelengths (i.e., $P_{\text{Da}}[\lambda_C] > P_{\text{Da}}[\lambda_F]$).

At the near focus, the power of the bifocal lens P_N becomes the addition of both the refractive base power and the diffractive add power, that is $P_N = (P_R + P_{\text{Da}})$, and so does its variation with the wavelength $\Delta P_N(\lambda) = \Delta P_R(\lambda) + \Delta P_{\text{Da}}(\lambda)$. In equivalent terms,

$$\text{LCA}_N = \Delta P_N(\lambda) = \text{LCA}_D + \Delta P_{\text{Da}}. \quad (5)$$

For example, assuming $\lambda_0 \approx \lambda_d$ and $\Delta\lambda = \lambda_C - \lambda_F$, the total chromatic aberration at the near focus (LCA_N) would be $\text{LCA}_N = \text{LCA}_D - ([\lambda_C - \lambda_F] / \lambda_D)P_{\text{Da}}(\lambda_D)$, where LCA_D would be computed using Equations 2 and 3. As mentioned, the chromatic aberration produced by a diffractive component (Equation 4) increases rapidly with wavelength and is opposite the chromatic aberration produced by a refractive element (Equation 2). Equation 5 suggests that a potential compensation of the LCA, totally or in part, can occur in the near focus of a diffractive 2f-IOL. This is not possible in the distance focus, for which only the refractive component of the lens contributes (Equations 2 and 3). So far, we have analyzed how the LCA affects the distance and the near foci of a single diffractive 2f-IOL. To further illustrate how it contributes to the whole chromatic aberration of the human eye in the distance and near vision, the dispersive characteristics of other ocular media need to be considered. This step forward will lead us, as discussed in the Results section, to use a pseudophakic schematic eye to simulate the LCA that would eventually affect the retinal image.

Through-Focus Energy Efficiency of a Refractive–Diffractive Bifocal Lens

The image formation of a diffractive 2f-IOL has been described as a combination of 2 images: the focused image produced by one of the IOL powers surrounded by a blur (halo) that corresponds mainly to the overlying on-axis out-of-focus image produced by the other power. For an insight concerning a geometrical explanation of such compound image, the mathematical description of its characteristics, halo formulae, and experimental intensity profiles obtained for a variety of multifocal IOLs, the interested reader is referred to other studies (see Refs. 13 and 14).

The TF-EE is the measure of image quality we used in this work to test the diffractive 2f-IOLs with the R, G, B lights. It is worth remarking that the energy efficiency (EE) values of the distance and near foci are straightforwardly obtained from dense sampling of the through-focus measurement, particularly in the axial neighborhood of such focal planes. The same test was repeated for the reference 1f-IOLs, but referred only to their single (distance) focus.

A method to measure the EE in the image space has been reported in detail for 1 or more wavelengths.[3,4] It assumes a pinhole object at infinity and a charge-coupled device (CCD) camera with linear response for digital image acquisition. The method first applies an edge-detection algorithm to segment the central core of the pinhole image at the focus plane of the lens (either the distance or the near focus in a 2f-IOL) and quantifies the amount of light intensity in the core (I_{core}) relative to the intensity in the full image that comprises the core and the background ($I_{\text{total}} = I_{\text{core}} + I_{\text{background}}$). The ratio $\eta = I_{\text{core}} / I_{\text{total}}$ is easy to compute in the experimental practice and approaches the so-called light-in-the-bucket metric[15] used (see Ref. 2) to quantify the polychromatic image quality of 1f- and 2f-IOLs by numerical simulation. For a through-focus analysis, the core contour determined in the best focus plane is applied unchanged to the defocus images obtained by axial scanning of neighbor planes. In 2f-IOLs, this axial scanning stretches to cover the distance and the near foci, thus allowing us to plot the TF-EE between them.

In this work, a TF-EE curve is experimentally obtained for each IOL under study with a fixed pupil size and for every R, G, and B light. Measurements were taken in the IOL image space, with the origin of vergences (0 D) set at the distance image for the G light (530 ± 15 nm, the closest to the design wavelength

Investigative Ophthalmology & Visual Science

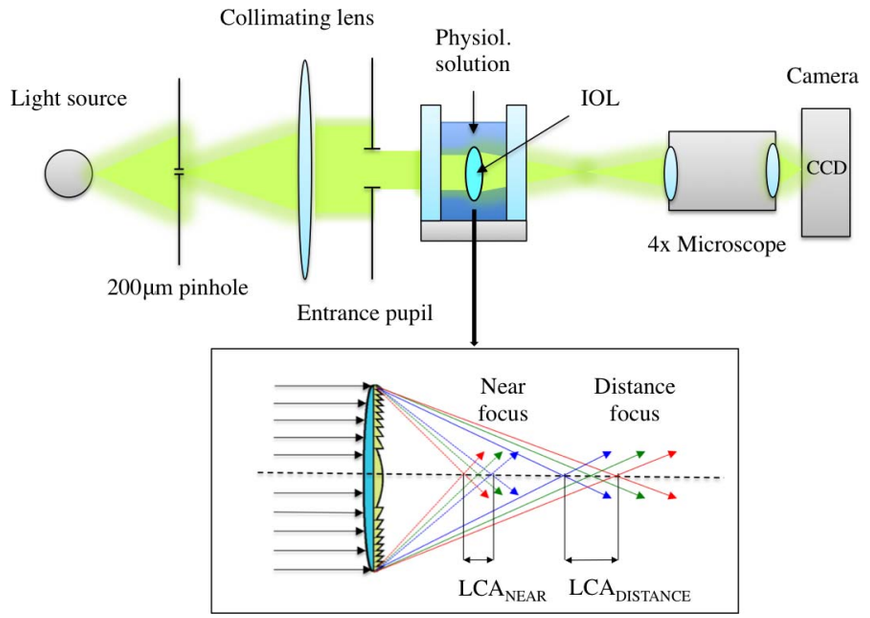

Figure 1. Experimental setup. The inset shows the LCA affecting the distance and near foci behind a diffractive 2f-IOL.

of 546 ± 10 nm, with full width at half maximum [FWHM] not greater than 20 nm).[16] The through-focus maximum intervals covered 7 D for 2f-IOLs and 4 D for 1f-IOLs in 0.2-D steps, and LCA experimental values were obtained from the power difference between the extreme EE peaks (usually the R and B peaks, but not necessarily) at each focus plane (i.e., LCA_D and LCA_N for 2f-IOLs and just LCA for 1f-IOLs).

Experimental Setup

The experimental work of this study has been done using the setup sketched in Figure 1. This setup is similar to others containing an ISO eye model[16] in an optical bench already described in detail and used in former works,[4] except for the artificial cornea, which has been removed in this study. Three R, G, and B LEDs (Thorlabs, Inc., Newton, NJ, USA)[17] with nominal wavelengths (NW) and FWHM, detailed in Table 2, were sequentially used to illuminate the setup. A 200-µm pinhole test object was placed at the front focal plane of a collimating lens of 200-mm focal length. The collimated beam illuminated the wet cell where the IOL was inserted, and thus either 1 or 2 aerial images of the pinhole object were formed behind the wet cell by the 1f- or the 2f-IOL, respectively. A diaphragm, placed in front of the wet cell and used as entrance pupil, limited the IOL aperture to 3.5-mm diameter throughout the experience. The amounts of negative SA of all the tested IOLs were limited accordingly. Behind the wet cell, an infinite corrected microscope mounted in a translation holder focused the aerial image of interest and magnified it onto a monochrome 8-bit CCD camera used for digital image acquisition. The set of microscope and camera could be moved along the bench axis to locate the best focal planes for each IOL and observation distance, with a spatial resolution of ±1 µm. The microscope objective (4× Olympus Plan Achromat; Olympus, City, ST and/or Country) had diffraction-limited performance through the visible spectrum and was specifically designed for high-quality imaging applications. For every IOL and wavelength, the intensity of the LED source and the time integration of image acquisition were adjusted to obtain a linear response of the camera in the intensity range of the aerial images (from distance to near images) with no saturation of the camera sensor. ?10

Table 2. Data of the Thorlabs Red (R), Green (G), and Blue (B) LEDs Used to Illuminate the Experimental Setup (Fig. 1)[17]

LED	Manufacture Model	NW, nm	FWHM, nm
B	Thorlabs M455L3	455	±10
G	Thorlabs M530L3	530	±20
R	Thorlabs M625L3	625	±10

For LEDs in the visible spectrum, the NW indicates the wavelength at which the LED appears brightest to the human eye. The NW for visible LEDs may not correspond to the peak wavelength as measured by a spectrograph.

In a closely related work,[2] the authors estimated by numerical simulation an imaging quality metric, namely the light-in-the-bucket metric, because of its ability to capture the property of IOL efficiency as well as image blur. They computed through-focus light-in-the-bucket curves to simulate the EE and energy distribution of several IOLs under R, G, B lights. As stated by the authors, "this metric quantifies the total amount of light in the central core of the point spread function (PSF) relative to that in a monofocal diffraction-limited PSF for the same wavelength and pupil size."[2] To implement this metric in practice, the ideal point source is substituted by a pinhole of certain size. We have used a 200-µm pinhole test object, which allows us to have enough energy in the image space to develop the whole experiment, and have computed the ratio $\eta = I_{core} / I_{total}$ according to the aforementioned procedure.[4] A misclassification error occurs in each focal plane due to the central part of the out-of-focus image, which overlays the bucket, thus contributing to the energy efficiency of the in-focus image. This misclassification error can be roughly approximated by the ratio of areas,

$$\text{error } (\%) = \frac{\text{area of the bucket}}{\text{area of the out-of-focus image}} \times 100 \quad (6)$$

The area of the bucket is the diffracted image of the pinhole, and the size of the out-of-focus image area is calculated using basic geometry. For the 2f-IOLs of our study,

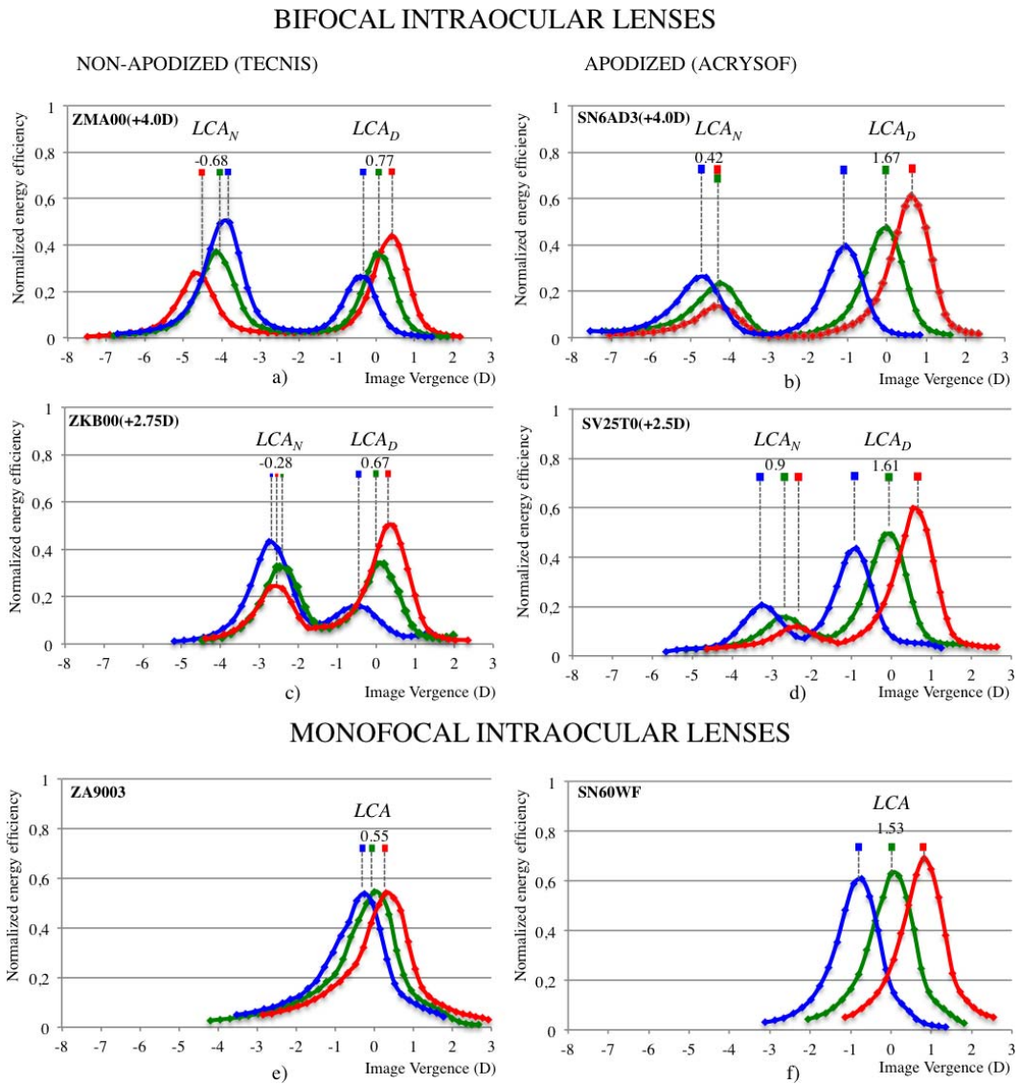

Figure 2. Experimental measurement of EE, through-focus energy distribution, and LCA in the tested 2f-IOLs and 1f-IOLs.

the highest error corresponds to the lens with the lowest add power (+2.5 D) and is about 3% in both the near and the distance focal planes.

RESULTS

Through-Focus Energy Efficiency

Figure 2 shows the experimental TF-EE measured for all the studied 1f- and 2f-IOLs with the 3 R, G, B lights, using the implementation of the light-in-the-bucket metric described in previous sections. Energy efficiency values have been normalized to unity for each wavelength and lens.

Bifocal IOLs show a double set of R, G, B EE peaks that correspond, as expected, to the distance and the near foci. Monofocal IOLs have, in turn, a single set of R, G, B EE peaks that correspond to their single focus intended for distance vision. A relative displacement of R, G, B plots for every focus and IOL accounts for the existing LCA, which is discussed below. Figure 2 shows that the distribution of the energy between the distance and the near foci of diffractive 2f-IOLs depends on the IOL design (apodized vs. nonapodized IOLs). The energy deflected and focused on the zero and first diffraction orders (distance and near focus, respectively) is balanced when the distance and near EE peaks reach similar height. For the pupil size of 3.5 mm used in our experiment, the distance and near EE peaks are more balanced with nonapodized than with apodized 2f-IOLs. For instance, with the ZMA00 (+4 D) lens (Fig. 2a), we obtain 0.36 distance and 0.37 near EE peak values for the G light, whereas with SN6AD3 (+4 D) lens (Fig. 2b), we obtain 0.47 distance and 0.23 near EE peak values for the same G light. The latter class (apodized AcrySof ReSTOR 2f-IOLs) shows clear energy predominance of the distance focus over the near focus, which is in agreement with the apodized design of these lenses aimed at preventing deleterious glare and halos in distance vision, particularly in dimmer mesopic illumination.[10]

Additionally, 2f-IOLs with lower add power (higher add f number), such as SV25T0 +2.5 D and ZKB00 +2.75 D, are slightly less efficient in the near focus—with all 3 R, G, B wavelengths—than lenses with higher add power (lower add f number), such as ZMA00 +4 D and SN6AD3 +4 D. For instance, in the near focus of the SV25T0 (+2.5 D) lens (Fig. 2d), the {R, G, B} EE peaks reach the values {0.12, 0.16, 0.20}, whereas in ?11

?16

Table 3. Values of LCA at the Distance and Near Foci of 2f-IOLs and at the Single Focus of 1f-IOLs

IOL	LCA Distance			LCA Near			
All of 30-D base power	ΔP_R\{FdC\}	Experim ΔP_R\{RGB\}	$[LCA_D]_{Eye}$	ΔP_{Da}\{RGB\}	ΔP_R\{RGB\} + ΔP_{Da}	Experim LCA_N	$[LCA_N]_{Eye}$
TECNIS							
ZMA00 Bifocal+4	0.57	0.77	1.99	−1.26	−0.49	−0.68	0.54
ZKB00 Bifocal+2.75	0.57	0.67	1.89	−0.87	−0.20	−0.28	0.94
ZA9003 Monofocal	0.57	0.55	1.77				
ACRYSOF							
SN6AD3 Bifocal +4	1.24	1.67	2.87	−1.26	0.41	0.42	1.62
SV25T0 Bifocal +2,5	1.24	1.61	2.80	−0.79	0.82	0.90	2.10
SN60WF Monofocal	1.24	1.54	2.73				

All data are in diopters. ΔP_R\{FdC\}, calculated with Equation 2, is LCA for distance (LCA_D of 2f-IOLs). Experim ΔP_R\{RGB\} is the experimental measurement of LCA with the R, G, B LEDs for distance. ΔP_{Da}\{RGB\}, calculated with Equation 4, is LCA due to the diffractive add power of 2f-IOLs. Experim LCA_N is the experimental measurement of LCA with the R, G, B LEDs for near vision. $[LCA_D]_{Eye}$ and $[LCA_N]_{Eye}$ are the simulated values of LCA in Le Grand pseudophakic schematic eye for distance and near vision.

the same focus of SN6AD3 (+4 D) lens (Fig. 2b), they reach the values {0.13, 0.23, 0.26}.

More importantly, the distribution of energy between the foci also depends on the illumination wavelength as already described[2,8] based on the dependence of the diffraction efficiency with wavelength.[18,19] Our experimental results in Figure 2 confirm the basics of those predicted by Ravikumar et al.[2] using numerical simulations, but they also disclose important differential features between the IOLs under study. Thus, in the near focus of all tested 2f-IOLs, our experiments coincide with theirs in obtaining higher (lower) EE for the blue (red) light than for the design wavelength (546 nm, close to our 530 nm light). Conversely, the opposite effect occurs in the distance focus, for which lower (higher) EE for the blue (red) light than for the design wavelength can be acknowledged.

Longitudinal Chromatic Aberration Table 3 shows the values of LCA in the distance and near foci of the set of diffractive 2f-IOLs, as well as in the single focus of the 1f-IOLs (the latter intended exclusively for distance vision) obtained in two different ways:

1. From the experimental position of all EE peaks in the optical setup accounting for the distance, near, and single powers of the set of IOLs under the sequential illumination of the R, G, and B lights (see LCA_D, LCA_N, and LCA labels in Fig. 2).
2. By numerical estimation. We have used Equation 2 to compute the $LCA_D = \Delta P_R$\{FdC\} with the data of refractive index, Abbe value, and IOL base power contained in Table 1. To calculate $\Delta P_{Da}\{\lambda\}$ (Equation 4), we have used the IOL add power (Table 1) and the R and B NWs of the LED sources utilized in the experimental setup (Table 2). For a closer estimation of LCA_N with Equation 5, we have used the experimental measures of $LCA_D = \Delta P_R$\{RGB\} obtained with the RGB lights instead of the computed values of $LCA_D = \Delta P_R$\{FdC\}.

In addition, to better illustrate the LCA effects produced by a given IOL when it is implanted in a human eye, we have simulated the resultant LCA in a model eye for the specific R, G, B wavelengths used in the experiment. To this end, we have considered Le Grand pseudoaphakic schematic eye,[6,20] along with the chromatic dispersions of the ocular media (cornea and aqueous humor) determined with Cauchy's equation[21] and the coefficients provided by Atchison and Smith[22] (data contained in Supplementary Table S1). Using the powers measured experimentally (Fig. 2), the LCA was computed in the distance and the near foci of Le Grand pseudoaphakic schematic eye for all the IOLs.

Regarding the LCA in distance due to the IOL immersed in the wet cell, the estimated values ΔP_R\{FdC\}predict constant positive LCA_D for 1f- and 2f-IOLs of the same material and base power (first left column in Table 3). For the AcrySof lenses, they are about twice the values of the Tecnis lenses, which is consistent with the higher dispersion of AcrySof material (lower Abbe value). The estimated values are in good agreement with the experimental values ΔP_R\{RGB\} (second left column in Table 3), but somewhat lower. This fact can be explained by the difference between the spectral wavelength ranges used for the numerical estimation $\{\lambda_F, \lambda_d, \lambda_C\}$ and the illumination of the experimental setup {B, G, R}. Although $\Delta\lambda =$ 170 nm in both cases, the extreme wavelengths do not coincide. Particularly in the blue region, the difference between the wavelength F (486 nm), used for numerical estimation, and B (455 nm), actually used to illuminate the setup, tends to increase the experimental LCA, more specifically for those materials with lower Abbe value (greater dispersion) such as AcrySof. The positive LCA_D value of every IOL combines with the positive LCA of the cornea in Le Grand pseudophakic schematic eye to produce greater aberration ($[LCA_D]_{Eye}$). In this sense, while the natural LCA of the human eye, in terms of the subjective chromatic difference of refraction, results approximately in 1.3 D for the spectral range considered in this work (455–625 nm),[20,23] the distance LCA of the pseudophakic eye with any of the Tecnis IOLs is larger than 1.3 D and becomes even worse in the case of the AcrySof lenses, with values of $[LCA_D]_{Eye}$ reaching 2.87 D (see values of $[LCA_D]_{Eye}$ in Table 3).

Regarding the LCA in near vision with diffractive 2f-IOLs, the add power variation ΔP_{Da}\{RGB\}, which is proportional to the add power, is calculated with Equation 4 (center column of Table 3). In all cases, the negative sign of ΔP_{Da} proves its compensating effect on the aberration introduced by ΔP_R\{RGB\} when both terms are totaled in the estimation of the LCA_N (Equations 3–5). The results obtained in this case are qualitatively different for the Tecnis and AcrySof 2f-IOLs (see third right column in Table 3). While LCA_N of Tecnis 2f-IOLs is finally negative (which means a reverse order in the wavelengths forming the near focus with respect to the order in the distance focus), LCA_N of AcrySof 2f-IOLs is finally positive (which means the same order in the wavelengths forming the near and the distance foci). The magnitude of LCA_N also deserves comment. The relatively low refractive power variation of 2f-Tecnis IOLs with wavelength is quickly surpassed by their diffractive add-power variation, for which, even in the case of the lowest add (ZKB00, add +2.75 D), LCA_N

Investigative Ophthalmology & Visual Science

results in a negative value (LCA_N[ZKB00] = −0.20 D). A larger amount of negative LCA is predicted for the ZMA00 Tecnis IOL, with +4 D add power (LCA_N[ZMA00] = −0.49 D). On the contrary, the relatively high refractive power variation of 2f-AcrySof IOLs with wavelength cannot be fully compensated by their diffractive add-power variation, for which, even in the case of the highest add (SN6AD3, add +4 D), LCA_N results in a positive value (LCA_N[SN6AD3] = 0.41 D). A larger amount of positive LCA is yet predicted for the SV25T0 AcrySof IOL, with +2.5 D add power (LCA_N[SV25T0] = 0.82 D). The experimental results of LCA_N, derived from the EE peak positions at near focus in Figure 2 and included in the second right column in Table 3, agree with these numerical estimations in both the sign and magnitude.

The experimental LCA_N of every IOL combines with the positive and higher LCA of the cornea to produce the final LCA in the near focus of Le Grand pseudophakic schematic eye ($[LCA_N]_{Eye}$) (first right column of Table 3). In all 2f-IOLs, it satisfies $[LCA_N]_{Eye} < [LCA_D]_{Eye}$, that is, there is certain compensation in the LCA of the near focus, but the compensation is accomplished considerably better by Tecnis (with only 0.54 D for ZMA00) than AcrySof 2f-IOLs. To further illustrate the difference, while Tecnis IOLs have $[LCA_N]_{Eye}$ values within the natural refractive error of 1.3 D for the same spectral range, AcrySof IOLs exceed this figure.

Discussion

We studied the LCA, analytically and measured experimentally, of 2 types of diffractive 2f-IOLs in their distance and near foci and have estimated their contribution to the LCA of the retinal image by numerical simulation in a pseudophakic schematic eye. For comparison, we have included 2 additional 1f-IOLs in our study. The distribution of energy between foci has been experimentally determined for every IOL under 3 R, G, B lights by means of through-focus measurements of the EE.

Our results, mainly contained in Table 3 and Figure 2, are consistent with other results obtained by numerical simulation in related works.[2,7,8] They analyzed numerically the design of hybrid diffractive–refractive IOLs inserted in a polychromatic pseudophakic model eye. For instance, an aspheric monofocal hybrid IOL, proposed by López-Gil and Montés-Micó,[7] has the diffractive surface intended to correct for the eye's LCA. In this lens, the diffractive profile directs nearly all the incoming light to its first diffraction order, where diffractive and refractive powers add up and, as a result, a single achromatic focal point is formed for distance object imaging in a modified Navarro et al. model eye.[20,24] Castignoles et al.[8] paid more attention to the diffractive element of multifocal IOLs, more specifically, to the influence of the phase profile function (binary, parabolic, sinusoidal) on the distribution of EE between the ± 2, ± 1, and 0 diffraction orders. They extended their simulation beyond the design wavelength (λ = 550 nm) to include the effects of chromatism in a simplified eye model consisting of a planar diffractive element against a perfect lens equivalent to the human eye. A step closer to our study can be found in the comprehensive work done by Ravikumar et al.,[2] who further included three different hybrid IOLs: monofocal, nonapodized bifocal, and apodized bifocal, in their polychromatic analysis of IOL performance. In their numerical simulations, the authors used a reduced eye model optimally focused for distance objects at the wavelength λ = 550 nm. The total refractive power of the reduced eye, coming from the combination of the cornea and the refractive portion of the hybrid IOL, was treated as corresponding to a single diopter at the cornea plane. An equivalent diffractive optical element at the corneal plane was computed to produce the same diffraction pattern on the retina as the physical diffractive profile virtually inserted in the IOL plane. Although the work reported by Ravikumar et al.[2] has provided a valuable basis for ours, some of their simplifications could not be assumed in our study. In particular, they assumed that the LCA of the Indiana eye chromatic model was a reasonable estimate for the LCA in pseudophakic eyes, thus neglecting the distinct contribution of different IOL materials (with different refraction index and dispersive characteristics) to the LCA of both the distance and near foci of the pseudophakic eye. As a consequence, they found in their simulations a uniform $[LCA_D]_{Eye} \approx 1.3$ D in eyes implanted with either Tecnis or AcrySof lenses. In contrast to their simulated results, the formula we derived and our experimental results (Table 3 and Fig. 2) prove the role that the refractive features of 1f-IOLs and diffractive 2f-IOL materials (i.e., refraction index and Abbe value) play in the LCA of their image focal planes. In this regard, we have shown that the $[LCA_D]_{Eye}$ may be significantly larger in the case of IOLs made of highly dispersive material, reaching values close to 3 D in distance vision. Moreover, we have also shown the influence of the refractive features of diffractive 2f-IOL materials on the achromatizing effect at near vision.

Conclusions

The distribution of energy between the near and distance foci of diffractive 2f-IOLs, as measured experimentally in an optical bench, proves to be different depending on the lens design, the illumination wavelength, and, to a lesser extent, the add power. In all the tested lenses, the experimental results of the TF-EE analysis agree with the characteristics expected from the IOL design.

In distance vision, diffractive 2f-IOLs (and 1f-IOLs) increase the positive LCA of prior ocular media. The more dispersive the IOL material (lower Abbe value), the greater is the LCA. With the tested IOLs implanted, the LCA of pseudophakic eyes would surpass even the natural chromatic aberration of the human eye.

In near vision, diffractive 2f-IOLs tend to reduce the amount of LCA. This achromatizing effect varies linearly with the add power and, depending on the IOL material and the amount of refractive LCA produced, may compensate, in part, the LCA of the eye in near vision. This fact benefits near vision in a pseudophakic eye implanted with a diffractive 2f-IOL.

Acknowledgments

Supported by project DPI2013-43220-R from the Spanish Ministerio de Economía y Competitividad y Fondos FEDER.

Disclosure: **M.S. Millán**, None; **F. Vega**, None; **I. Ríos-López**, None

No author has a financial or proprietary interest in any product, method, or material mentioned in this article.

References

1. Holladay JT, Piers PA, Koranyi G, Van der Mooren M, Norrby S. A new intraocular lens design to reduce spherical aberration of pseudophakic eyes. *J Refract Surg*. 2002;18:683–691.
2. Ravikumar S, Bradley A, Thibos LN. Chromatic aberration and polychromatic image quality with diffractive multifocal intraocular lenses. *J Cataract Refract Surg*. 2014;40:1192–1204. doi:10.1016/j.jcrs.2013.11.035.
3. Vega F, Millán MS, Vila-Terricabras N, Alba-Bueno F. Visible versus near-infrared optical performance of diffractive multifocal intraocular lenses. *Invest Ophthalmol Vis Sci*. 2015;56:7345–735. doi:10.1167/iovs.15-17664.

4. Vega F, Alba-Bueno F, Millán MS. Energy distribution between distance and near images in apodized diffractive multifocal intraocular lenses. *Invest Ophthalmol Vis Sci*. 2011;52:5695–5701. doi:10.1167/iovs.10-7123.
5. Vega F, Alba-Bueno F, Millan MS. Energy efficiency of a new trifocal intraocular lens. *J Eur Opt Soc Rapid Publ*. 2014;9:14002. doi:10.2971/jeos.2014.14002.
6. Le Grand Y. *Form and Space Vision*. Rev. ed. Millodot M, Heath G, trans. Bloomington, IN: Indiana University Press: 1967.
7. López-Gil N, Montés-Micó R. New intraocular lens for achromatizing the human eye. *J Cataract Refract Surg*. 2007;33:1296–1302. doi:10.1016/j.jcrs.2007.03.041.
8. Castignoles F, Flury M, Lepine T. Comparison of the efficiency, MTF and chromatic properties of four diffractive bifocal intraocular lens designs. *Opt Express*. 2010;18:5245–5256.
9. Alcon. Product information [webpage on the Internet]. Available at: http://www . Accessed December 10, 2015. ?12
10. Davison JA, Simpson MJ. History and development of the apodized diffractive intraocular lens. *J Cataract Refract Surg*. 2006;32:849–858. doi:10.1016/j.jcrs.2006.02.006.
11. Abbott Medical Optics. Product information [webpage on the Internet]. Available at: http://www.. Accessed December 10, 2015. ?13
12. Buralli DA, Morris GM, Rogers JR. Optical performance of holographic kinoforms. *Appl Opt*. 1989;28:975–983.
13. Alba-Bueno F, Vega F, Millán MS. Halos and multifocal intraocular lenses: origin and interpretation. *Arch Soc Esp Oftalmol* (English ed.). 2014;89:397–404. doi:10.1016/j.oftale.2014.10.002.
14. Pieh S. Halo size under distance and near conditions in refractive multifocal intraocular lenses. *Br J Ophthalmol*. 2001;85:816–821. doi:10.1136/bjo.85.7.816.
15. Thibos LN, Hong X, Bradley A, Applegate RA. Accuracy and precision of objective refraction from wavefront aberrations. *J Vis*. 2004;4:329–351. doi:10.1167/4.4.9.
16. International Organization for Standardization. *ISO 11979-2:2014 Ophthalmic Implants—Intraocular Lenses—Part 2: Optical Properties and Test Methods*. Geneva; ISO: 2014.
17. Thorlabs, Inc. Product information [webpage on the Internet]. Available at: http://www . Accessed December 10, 2015. ?14
18. Faklis D, Morris GM. Spectral properties of multiorder diffractive lenses. *Appl Opt*. 1995;34:2462–2468. doi:10.1364/AO.34.002462.
19. Turunen J, Wyrovski F. *Diffractive Optics for Industrial and Commercial Applications*. Berlin: Wiley Akademie Verlag; 1998.
20. Atchison DA, Smith G. *Optics of the Human Eye*. Oxford, UK: Butterworth-Heinemann; 2000: 184.
21. Longhurst RS. *Geometrical and Physical Optics*. 3rd ed. London, Longman; 1973: 500.
22. Atchison DA, Smith G. Chromatic dispersions of the ocular media of human eyes. *J Opt Soc Am A*. 2005;22:29–37.
23. Thibos LN, Ye M, Zhang X, Bradley A. The chromatic eye: a new reduced-eye model of ocular chromatic aberration in humans. *Appl Opt*. 1992;31:3594–3600.
24. Navarro R, Santamaría J, Bescós J. Accommodation-dependent model of the human eye with aspherics. *J Opt Soc Am A*. 1985;2:1273–1281.

Investigative Ophthalmology & Visual Science

Queries for iovs-57-04-15

1. **Author: This article has been lightly edited for grammar, style, and usage. Please compare against your original document and make changes on these pages. Please limit your corrections to substantive changes that affect meaning. If no change is required in response to a question, please write "OK as set" in the margin. Copy editor.**
2. **Author: Short title "Polychromatic Image Performance of Diffractive 2f-IOLs" created for the running header per journal style. Please confirm the wording. Copy editor**
3. **Author: In the abstract, in the sentence beginning "Four aspheric 2f-IOLs (Tecnis +4.00 D ZMA00," does "add" mean "additional," as it is used in the body of the article and as edited? Copy editor**
4. **Author: Math in this article set by compositor; please check carefully. Copy editor**
5. **Author: Carefully check the spelling and order of the author names and check the affiliations for all of the authors.**
6. **Author: Make sure that ALL funding/financial support is listed in the information following the Acknowledgments.**
7. **Author: Edited Equation 1 to use delimiter order ([ ]) per journal style. Please confirm the equation is correct. Copy editor**
8. **Author: Edited equation 2 to use delimiter order ([ ]) per journal style. Please confirm the equation is correct. Copy editor**
9. **Author: In the sentence beginning "It assumes a pinhole object," has CCD been expanded correctly as charge-coupled device? Copy editor**
10. **Author: In the sentence beginning "The microscope objective," please provide the full manufacturer name and the city, state and/or country of location per journal style. Copy editor**
11. **Author: In the sentence beginning "Additionally, 2f-IOLs with lower add power (higher add f number)," please expand "f" at first use. Copy editor**
12. **Author: For reference 9, please supply the URL at the placeholder. Copy editor**
13. **Author: For reference 11, please supply the URL at the placeholder. Copy editor**
14. **Author: For reference 17, please supply the URL at the placeholder. Copy editor**
15. **Author: In Table 1, should "UV and blue light" be "UV blocking and blue light? Also, correct that some of the empty table cells have dashes and some do not? Copy editor**
16. **Author: In Table 3, changed "$LCA_{Distance}$" and "LCA_{Near}," to LCA Distance and LCA Near to avoid confusion with "LCA_D" and "LCA_N". Okay? Copy editor**